

Evaluation of Linear and Comminuted Bone Fracture Status by using One Dimensional Ultrasound System

Maheza I. Mohamad Salim, Alwin A. Alexander, Sallehuddin Ibrahim and Eko Supriyanto.

Abstract— This paper presents a method for the evaluation of linear and comminuted bone fractures by using one dimensional ultrasound system. This paper includes an investigation on the attenuation of 1 MHz ultrasound wave propagating through a normal and fractured bone, through utilising the pulse echo method. Two types of bone fracture were included in this study, namely the linear fracture and comminuted fracture, which were simulated using a goat's bone encased in gelatin. The reflected echoes were analysed to determine the power spectral density and ultrasound attenuation based on insertion loss method. The ultrasound attenuation resulting from a normal and fractured bone showed that average signal power on the fractured bone was lower than the normal bone by 4.3dB for both linear and comminuted fractures. In addition to that, this study also shows that one dimensional ultrasound can be used to determine the fracture site precisely by observing the difference in ultrasound attenuation value. The fracture site was observed having higher ultrasound attenuation due to the presence of spaces and gaps that allowed the ultrasound to pass through it and further attenuated. Based on the result, the ultrasound signal attenuation showed a potential for use to detect bone fracture; nevertheless, further studies are still needed to determine the type of fractures. The present finding shows the potential of one dimensional ultrasound as a simpler and safer method in diagnosing bone fracture as an adjunct to x-ray imaging, especially for pregnant mothers and paediatric cases.

Keywords— Bone fracture, linear, comminuted, one dimensional ultrasound, attenuation.

Maheza I. M. Salim is a Senior Lecturer at the Department of Clinical Sciences, Faculty of Biosciences and Medical Engineering. She is also a member of Diagnostic Research Group and UTM-IJN Cardiovascular Engineering Center, Universiti Teknologi Malaysia, 81310 Johor Bahru, Johor, Malaysia (+60197646095), (e-mail: maheza@biomedical.utm.my).

Alwin A Alexander is currently a Product Development Engineer, Intel Microelectronics Sdn. Bhd. This research work was carried out when he was with Faculty of Electrical Engineering, Universiti Teknologi Malaysia, 81310 Johor Bahru, Johor, Malaysia.

Sallehuddin Ibrahim is an Associate professor at the Faculty of Electrical Engineering, Universiti Teknologi Malaysia, 81310 Johor Bahru, Johor, Malaysia.

Eko Supriyanto is a Professor and Director of UTM-IJN Cardiovascular Engineering Center, Universiti Teknologi Malaysia, 81310 Johor Bahru Malaysia.(email: eko@biomedical.utm.my)

I. INTRODUCTION

BONE fracture is among the most common musculoskeletal injuries and represents considerable global health burden every year [1]. Recent reports published that bone fractures take up one of the most frequent non-fatal injuries worldwide [2-3] with the most significant morbidity in childhood and elderly [4-5]. Other than that, the number of hip fractures worldwide was estimated to be 1.66 million worldwide in 1990 and is expected to increase to 6.26 million cases by 2050 [7-8]. The estimation has made World Health Organization (WHO) to call for increasing focus in managing musculoskeletal injuries worldwide. Hence, predicting, preventing and managing bone fracture are very crucial due to its high frequency, surgical complications and socioeconomic impact [7].

A. Anatomy and Physiology of the Bone and Bone Fractures.

The main role of the skeletal system is to provide structural support of the body, leverage and movement as well as protection for vital organs. It also performs other important functions such as for mineral reservoir and blood production [7]. The bone is a composite structure composed of hydroxyapatite, collagen, noncollagenous protein, water and small amount of proteoglycans [9-11]. However, these compositions vary according to species, age, sex and the specific bone itself [12]. Generally, bone tissue is nonhomogenous, porous and anisotropic. There are two types of bone tissue, namely the trabecular and cortical, which are distinguished according to their porosity. The trabecular bone has 50-95% porosity. This type of tissue is usually found in cuboidal bones, flat bones and at the ends of long bones. Pores in trabecular tissue are interconnected and filled with marrow for blood production [13]. On the other hand, the cortical bone has 5-10% of porosity. It is usually found in the shaft of a long bone and it surrounds the trabecular bone forming a flat bone.

Bone fractures are medical condition in which there is an incomplete or complete break in the continuity of the bone [14]. The break may be a result of a sudden injury due to high force impact and continuous stress as well as fragility due to osteoporosis or certain medical conditions that weaken the

bones, such as bone cancer. There are many types of bone fractures. The most common bone fractures include the greenstick, linear/fissured, and comminuted fractures. Greenstick fractures are incomplete fractures that cause the bone to bend, whereas comminuted fractures are characterized by fractures in which the bone fragments into several pieces. The linear/fissured fracture represents a fracture that is parallel to the bone's long axis. Figure 1 shows the condition of the three most common fractures, which are the greenstick, linear/fissured and comminuted bone fracture.

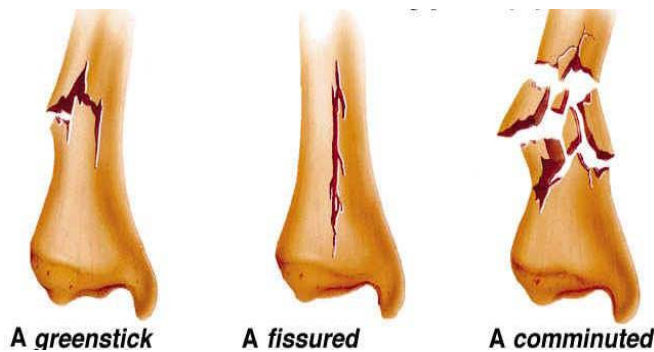


Figure 1: Types of bone fractures [6]

B. Current Diagnosis of Bone fracture

In clinical setting, radiographic x-ray is often performed as gold standard in the diagnostic of bone fracture [15]. Radiographic imaging involves exposing the fracture part to a small dose of ionizing radiation to get the image mapping [15-16]. Whilst radiographic imaging provides a clearest and most detail view of bone, it provides little information about muscle, tendons and joints. In situations where radiographic x-ray alone is insufficient, a Computed Tomographic scan may be performed, especially for the assessment of complicated and subtle fractures and dislocations [17]. However, the use of radiographic x-ray and CT in diagnostic of bone fracture is limited to certain group of patient, such as pregnant women due to x-ray radiation risk. Hence, an alternative diagnostic method which is safe, less time consuming, accurate and inexpensive is utterly needed. In this study, bone fracture evaluation by using one dimensional ultrasound is proposed.

Ultrasound is defined by sound wave having frequency in the range higher than 20KHz [18]. In medical setting, the ultrasound with frequency range of 1 MHz to 20 MHz is used as a diagnostic tool because it can be focused into small, well-defined beams that can probe the human body and interact with the tissue structures to form images. In general, ultrasound offers real time imaging which is safe from radiation, non-invasive, highly portable and inexpensive imaging modality [14, 22-23]. There are various dimensions of ultrasound imaging used in diagnostics. The most popular one is the 2D Ultrasound [24]. The 2D technology allows a cross sectional image of the anatomical mapping to be captured real time, and the most common application of this technology is

for abdominal diagnosis as well as Obstetric and Gynecologic Scanning. Nowadays, advancement in ultrasound technology has enabled 3D and 4D ultrasound to capture volumetric anatomical images [25]. 1D ultrasound is the least commonly used in medical setting due to inability of this system to produce image mapping. 1D ultrasound produces only ultrasound signal in x and y planes. The y plane corresponds to the wave intensity whilst the x plane corresponds to the propagation time or wave travelling distance. Although its usage is limited, 1D ultrasound offers simple and fast processing time as well as accurate diagnosis for certain medical cases [26].

The current application of ultrasound for bones is mainly for therapy such as healing bone fracture [19-20] and measuring bone mineral density [21]. So far, ultrasound is not primarily used for bone imaging because of the high acoustic impedance between the soft tissue and bones that renders difficulties for ultrasound signal to penetrate the bone. The ultrasound wave propagates as a pressure wave in any medium including the human body. In ultrasound machine, an ultrasonic transducer contains one or more elements made from a piezoelectric ceramic which converts the electrical signal into vibrations in ultrasonic frequency range.

Ultrasound attenuation occurs when the ultrasound pulse loses its mechanical energy continuously as it travels through anatomical structures. It is characterized by the reduction in amplitude and intensity as the wave propagates through the bone sample [27]. It encompasses the absorption as it travels, reflected and scattered as it encounters tissue interfaces and gelatin. Ultrasound reflection rate depends on the acoustic impedance difference between 2 tissue interfaces. Higher acoustic impedance difference will cause high probability of the signal to be reflected back. Scattering and refraction interactions also remove some of the energy from the ultrasound wave. However, the reduction of the energy is mainly due to the absorption process by the material and conversion into heat due to friction [28]. The rate at which an ultrasound pulse is absorbed depends on the material it passes through, and the frequency of the ultrasound. Lower density tissue will absorb more ultrasound energy compared to a higher density tissue [26]. Other than that, the attenuation rate is also affected by the frequency of ultrasound wave where the higher the frequency, the higher the attenuation will be, thus, giving less depth of penetration into the tissue. The ultrasound attenuation rate is specified in term of an attenuation coefficient in unit of decibels per centimeter (dB/cm). Since the attenuation in tissue increases along with frequency, it is necessary to specify the frequency when an attenuation rate is given.

In this study, a one dimensional ultrasound system at frequency of 1MHz was used to investigate and evaluate the status of bone fractures by analyzing its attenuation level. Our hypothesis is the fracture area will have higher attenuation compared to the normal area since the presence of fractures in the bone will introduce gaps and spaces that allow the

ultrasound wave to pass through the bone and be further attenuated. Unlike the fractured area, the normal area of the bone will experience lower attenuation due to the high acoustic impedance difference between soft tissue and bone that causes the sound wave to be reflected with less attenuation.

II. MATERIALS AND METHOD

A. Experiment Samples

Two goat's bones were used as samples in this study. The bones were cleaned and bleached with hydrogen peroxide to remove any bad odour, as shown in Figure 2. The bones were also encased in gelatine to stimulate soft tissue, as shown in Figure 3. Gelatin is used to stimulate soft tissue since the speed of ultrasound in gelatin is similar to soft tissues at approximately 1540m/s. Other than that, the composition of gelatin was designed to mimic the density of muscle around the bone. Each bone in Figure 2 was used twice in the experiment; firstly as normal bone sample, and then secondly as fractured bone sample. The fracture was simulated by applying appropriate force with blunt tool.

As shown in Figure 2, bone A was given a linear fracture, which is a fracture parallel to the bone's axis. Meanwhile, bone B was given a comminuted fracture, which is a fracture that causes the bone to fragment into a few parts as was described earlier in the introduction section. The different fractures tested were used to observe the feasibility of one dimensional ultrasound system to detect different fracture types.



Figure 2: Bleached normal bone sample



Figure 3: Bone encased in gelatin

B. Experimental Set Up and Measurements

The experiment set up consisted of a 5077PR One Dimensional, Manually Controlled Ultrasound Pulser Receiver unit, Olympus-NDT, Massachusetts, USA. The unit was set to deliver 400V of negative square wave pulses at the frequency of 1MHz to an ultrasound transducer with peak frequency at 1MHz. The transducer was used to transmit and receive the ultrasound wave in the pulse echo mode setting from the z direction. The pulser receiver was connected to a digital oscilloscope, and a laptop for display and storage purposes. Figure 4 and 5 show the block diagram and laboratory set up of the experiments.

After the measurement and recording stage, all data were processed to analyze power spectral density and attenuation coefficient using Matlab Software, Mathworks, Natick, USA. In the end, the final analysis was done in Microsoft Excel.

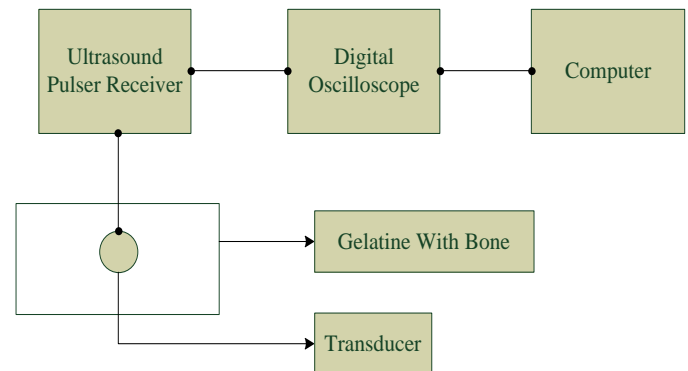


Figure 4: Top view Block diagram of experiment setup



Figure 5: Laboratory set up of the experiment

Data collection was done by taking 20 echo signals along the axis of the bone at an interval of 0.1cm, as shown in Figure 6. The transducer was placed on the top surface of the gelatin. After the first echo was recorded, the transducer was moved forward to 0.1cm and the data collection was repeated. The reading was taken 25 times for bone A and 20 times for bone B, for both normal and fractured condition. The ultrasound signal was first recorded from normal bone A and B. After completing the normal bone group, the bones were fractured and another cycle of ultrasound signal was recorded for the fractured bone group.

The collected data were categorized into 2 groups. Group 1 was labeled as normal bone and group 2 was labeled as fractured bone. Table 1 below summarises the grouping.

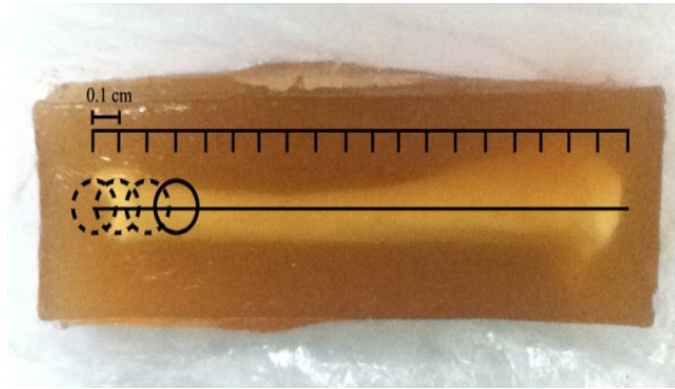


Figure 6: Scanning steps of ultrasound transducer

Table 1 : Bone sample grouping

	Normal	Fractured
Bone A	No fracture	Linear fracture
Bone B	No fracture	Comminuted fracture

C. Data Analysis

Each echo signal from normal and fractured group was stored in a computer as CSV file for analysis. In general, the processing steps involved the determination of frequency content of an ultrasound waveform via frequency decomposition to find its power spectral density and attenuation coefficient by using the Insertion Loss method as described elsewhere previously [29-32]. In the Insertion Loss method, the attenuation of material under test is determined by subtracting the energy of ultrasound travelling through the normal bone with the energy of ultrasound travelling through the fractured bone.

Firstly, the ultrasound signal in time-domain was converted into frequency domain by using the Fast Fourier Transform (FFT) algorithm. Following that, the signal was filtered and the power spectral density was calculated using the following formula: Given a signal X with N sampling, its power spectrum was calculated as follows for double sided spectrum.

$$\text{Power spectrum } S_{AA} = \frac{\text{FFT}(X) \cdot \text{FFT}^*(X)}{N^2} \quad (1)$$

where $\text{FFT}^*(A)$ denotes the complex conjugate of $\text{FFT}(A)$. To form the complex conjugate, the imaginary part of $\text{FFT}(A)$ was negated. The power values are in squared amplitude, therefore they were converted to dB scale which was more suitable to view wide dynamic ranges. The following formula can be used for conversion:

$$P(\text{db}) = 10 \log_{10} S_{AA} \quad (2)$$

Once the power densities for both normal and fractured bone were determined in decibel unit, the attenuation scale was calculated by subtracting the signal's power in dB for normal bone with the signal's power in dB for fractured bone. The equation for the attenuation is as follows:

$$\text{Attenuation (dB)} = P_N - P_F \quad (3)$$

where P_N is the signal's power for normal bone and P_F is signal's power for fractured bone.

The analysis was further done using the statistical approach. The power readings were loaded into Microsoft Excel to perform the statistical analysis of mean and standard deviation for all the groups as mentioned in Table 1.

III. RESULT AND DISCUSSION

A. Ultrasound Signal Processing

Data analysis was done in Matlab to calculate the attenuation coefficient of the ultrasound signal. A typical echo signal was recorded during the experiment, as shown in Figure 7. The recorded signal contained 500 lengths of discrete data.

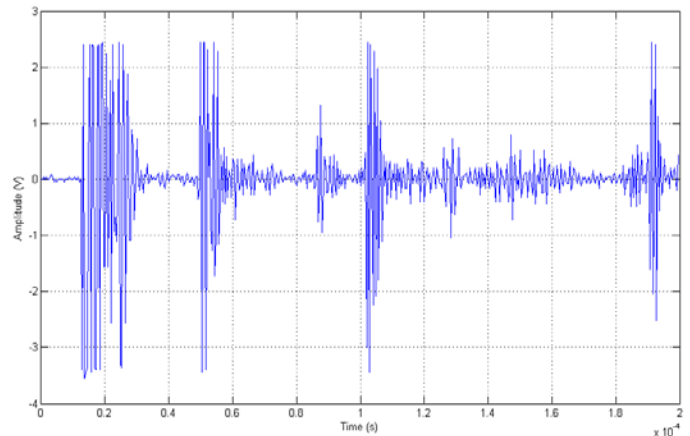


Figure 7: A typical echo signal recorded during the experiment.

From the signal, the identification process was done in order to determine the actual source of each echo. With the assumptions that ultrasound speed is constant, each echo distance was measured from the upper gelatin's surface to see the reflection sources. Signal identification was needed to select the necessary signal for further processing and to remove unwanted signal. The signal identification for the echo in Figure 7 is shown in Figure 8.

In Figure 8, the first peak that was recorded by the system represented the beginning of the echo signal that was first reflected at the upper gelatin's surface and sensed by the ultrasound transducer. The second and third peak represented the echoes that came out due to reflection at the bone's upper

and lower surfaces. These two echoes were followed by the last echo from the gelatin bottom's surface. Another small echo was also sensed from one of the lowest bone protrusions. The latter were the repetitions of the first five echoes with lower amplitude due to attenuation.

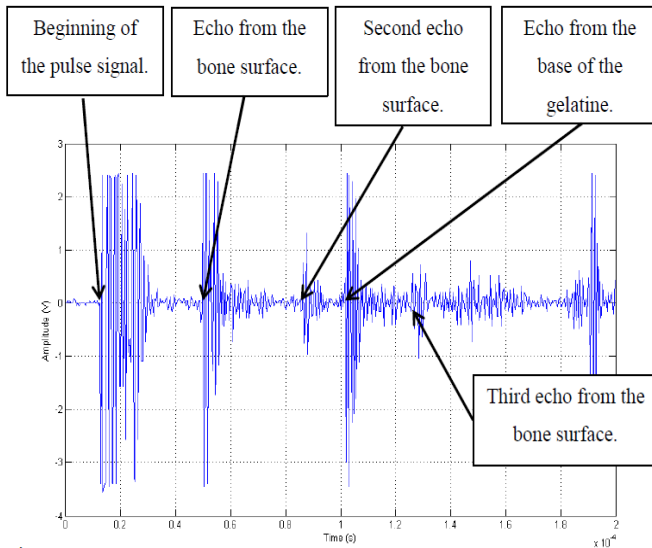


Figure 8: Echo signal identification

500 samples of data were obtained for each echo signal at the sampling frequency of 2.5MHz. This information was too long and the signal itself contained repetitive information in the end. Therefore, the signal was cropped so that only the necessary echo signal would be taken for power calculation. Data selection and extraction is very crucial in the processing stage to maintain calculation efficiency.

Figure 9 shows the extracted signal based on the 500 echo data in Figure 7. From the original signal, only the first 3 peaks were selected and extracted since they contained sufficient information with regard to the attenuation of ultrasound as it traveled through the bone sample. The total length of the extracted data contained 206 data samples.

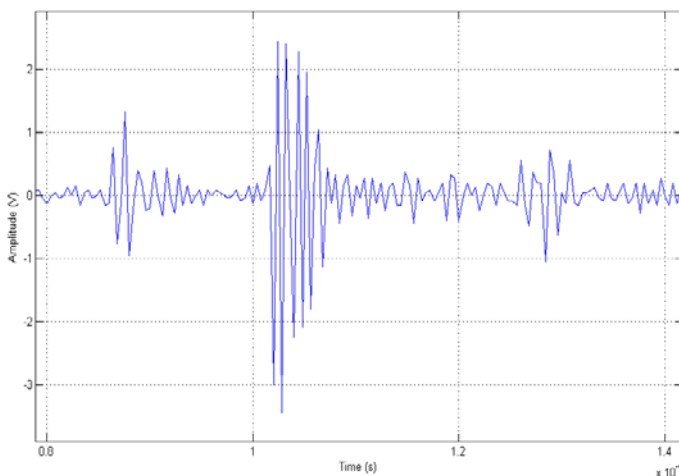


Figure 9: The extracted signal that contains 206 data samples is sufficient for power calculation

The extracted signal was then fed through a Fast Fourier Transform (FFT) algorithm so that analysis could be done in frequency domain. FFT was chosen for its high accuracy and fast computing time. The signal was then filtered using a 10th order Butterworth low pass filter with a 3dB cut-off frequency of 1.1MHz in Matlab signal processing toolbox. Butterworth filter was used because it would not cause ripples at the pass band although its roll-off rate was slower. To overcome that problem, a 10th order was chosen for the filter. Filtering involved the elimination of unwanted frequency higher than 1.1MHz to provide a smoothing effect to the signal after the elimination of high frequency signals.

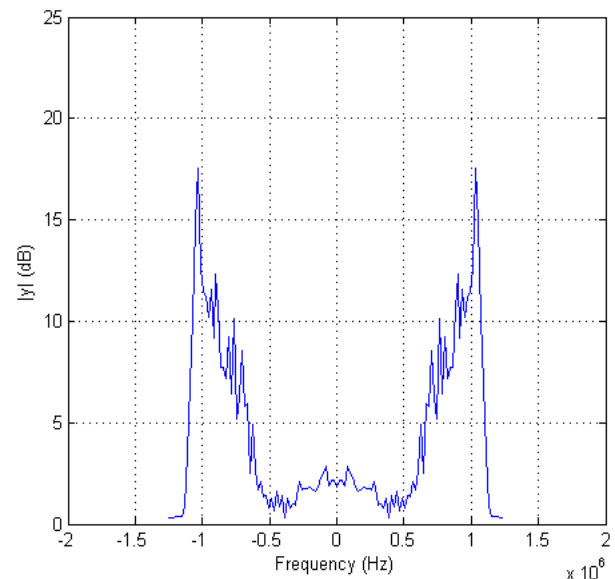


Figure 10: Ultrasound signal in frequency domain after the filtering process.

Figure 10 shows the ultrasound echo signal in frequency domain after the filtering process. From the figure, it can be seen that, the unwanted frequency components which was higher than 1.1MHz was removed after the filtering process, leaving only a very small amount that was very close to zero due to the gradual stopband property of the butterworth filter.

The spectral density of a wave, when multiplied by an appropriate factor, will give the power carried by the wave, per unit frequency, known as the power spectral density of the signal. PSD describes how the average power of a signal is distributed with frequency. In this study, the amplitude spectrum of an echo signal was obtained using the FFT algorithm. Based on the amplitude spectrum data, the power spectral density was calculated.

Using Equation 1 and 2 for calculating power spectral density, a graph was plotted, as shown in Figure 9. From there, the power of the signal at 1MHz could be retrieved.

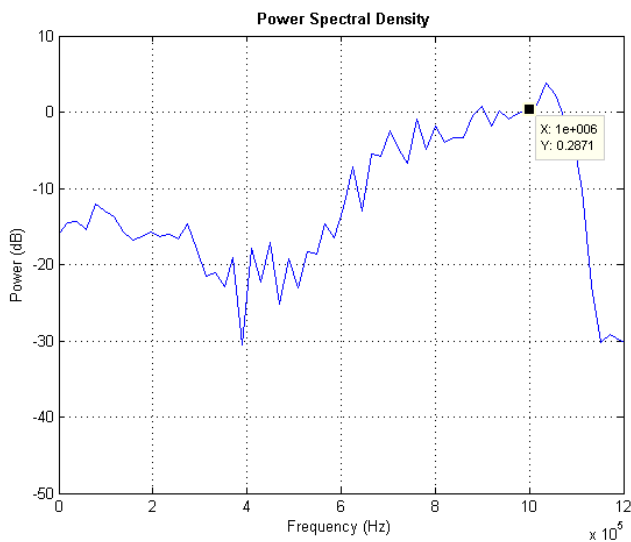


Figure 9: PSD of the ultrasound signal

Finally, the attenuation scale of ultrasound at 1MHz was determined from the slope of PSD plot.

B. Mean Ultrasound Attenuation for Normal and Fractured Bone

Table 1 below summarises the mean and standard deviation for ultrasound attenuation result for normal and fractured group.

Table 1 : Experiment result in the form of statistical data

	Bone A	Bone B
Normal (dB)		
Mean±stdev	-2.000±2.712	-9.419±3.625
Fractured (dB)		
Mean±stdev	-6.325±5.679	-13.807±5.549
Attenuation (dB)		
Mean±stdev	4.325±6.123	4.388±7.096

The result shows that the normal bone A and bone B had different signal power to begin with. Bone A had higher power at -2 dB whereas bone B had - 9.419 dB for its mean value. This significant difference of values for normal bones was due to the effect of the bone placement in gelatin. The placement for bone A was set nearer to the surface of the gelatin compared to bone B, which was placed slightly deeper into the gelatin. The ultrasonic signal might have been weakened through the absorption by the gelatin where the ultrasound signal through gelatin B suffered more absorption compared to gelatin A as the signal needed to travel deeper. This situation can be used to relate the attenuation, for example, scanning a fat person who has thick layers of fat or muscle compared to a skinny person with thin layer of fat. A higher attenuation can be observed during the scanning onto the fat person.

The standard deviation for both normal bones had no significant difference. The slight difference might be caused by the structural difference between bone A and bone B. The difference in shape and size should cause different reflections and scattering patterns for each bone [33].

Looking at the result of fractured bone, it could be clearly seen that the mean power value for both bones had decreased significantly. Absorption, scattering and reflection are the processes that contribute to ultrasound energy attenuation in tissue. Often, the resulting attenuation is a collective result of the three processes. However, many studies reported that, absorption is the most dominant factor contributing to attenuation of ultrasound wave in biological tissue via the relaxation energy loss [34-36].

In this experiment of analyzing fractured bone, absorption still plays the main role for the signal attenuation but the scattering and reflection processes of signal had increased due to the fractured state of the bone. Fractures introduced gaps and spaces into the bone which would cause the signal to penetrate even deeper. This would then increase the absorption process and attenuate more signals. Apart from that, fractures also caused substantial changes onto the structure of the bone. The alignment of the bone with the surrounding soft tissue would no longer be the same. This abnormal placement of fractured bone caused scattering and reflection that was directed were from the transducer, hence less signals were returned.

As seen in the result, the fractures had caused the signals to get weaker. However, based on the attenuation, the mean power values for both bone A and B were almost the same at 4.3dB, even though the two bones had different types of fractures.

In this experiment, it was found that power spectral density evaluation alone was insufficient to differentiate between linear and comminuted bone fracture. This was because the PSD gave the same value for different fracture types. Hence, a more complex algorithm is necessary for fracture differentiation and future studies will be focused on solving this issue. One possible explanation could be because the overall gaps and space produced in both fractures might be the same although the fracture classifications were different. This would eventually produce the same attenuation although the patterns of absorbing, reflecting and scattering signals were unique to each bone.

C. Determination of Fracture Site

The attenuation of ultrasound parallel to the bone axis was also plotted to investigate the capability of one dimensional ultrasound to determine the fracture site. The plot was made following the scanning step location as mentioned earlier in the methodology. During data collection, echo signals were recorded along the axis of the bone at the interval of 0.1 cm, as shown in Figure 4. The transducer was placed on the top surface of the gelatin. After the first echo was recorded, the transducer was moved forward to 0.1cm and the data collection was repeated. The reading was taken 25 times for bone A and 20 times for bone B. The resulting attenuation plot for normal and comminuted fracture bone are shown in Figure 10 and 12 respectively.

As can be seen in Figure 10, the range of attenuation for normal bone varied from -1dB to -12dB, depending on the location of the bone in the gelatin. The highest attenuation value was plotted at position A09-B02 which was the mid area of the bone.

This middle area was the farthest area from the gelatin surface, in which higher attenuation value was expected. The vertical distance of the mid area from the gelatin's surface is shown in Figure 11.

On the other hand, Figure 12 shows the ultrasound attenuation plot for bone with comminuted fracture. Overall, the attenuation pattern is similar with the normal attenuation pattern due to the shape and placement of the bone. However, the ultrasound attenuation value ranged higher between -2dB to -33dB with the highest value occurred at the fracture sited site. As discussed earlier, the fractures introduced gaps and spaces into the bone which would cause the signal to penetrate even deeper. This would then increase the absorption process and attenuate more ultrasound signals.

The results shown in Figure 10 and 12 have proven that one dimensional ultrasound can be used to determine the fractured site precisely by observing the difference in ultrasound attenuation value. It can be concluded that fracture site had higher ultrasound attenuation due to the presence of spaces and gaps that allowed the ultrasound to pass through it and be further attenuated.

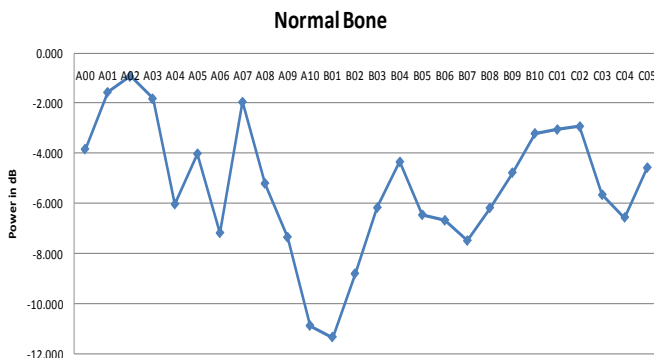


Figure 10: Graph of normal bone

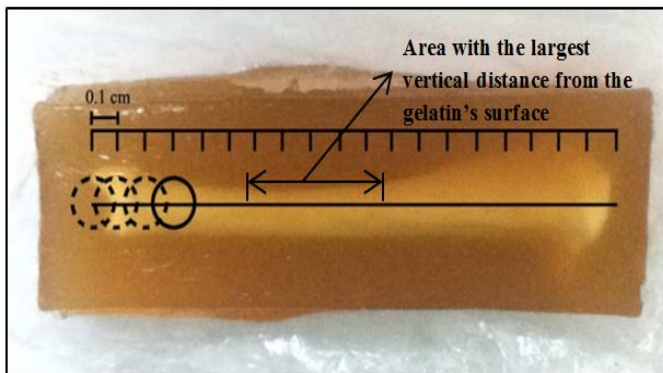


Figure 11: Bone vertical distance from gelatin's surface

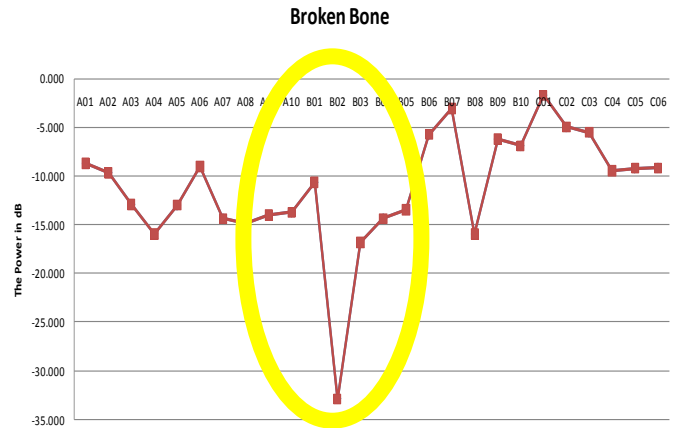


Figure 12: Graph of broken bone

Based on the research results, it has been proven that ultrasound attenuation can be used for bone fracture evaluation. Compared to other available evaluation methods such as x-ray, ultrasound does not use ionising radiation; plus, it is low cost and highly portable. The author used a single element ultrasound transducer along with an ultrasound pulser receiver for signal transmission, and data collection was made via a computer using a digital oscilloscope. The sample used comprised of two types of fracture, which were linear and comminuted fractures. The required signal was then extracted, filtered and the signal's power was computed. The power between the normal and fractured bone was compared to get the attenuation value. Based on the result, there was a significant amount of attenuation between the normal and fractured bone. Therefore, it has been proven that the attenuation of the signal can be used for fracture evaluation. However, the attenuation values for both type of fracture were the same, at 4.3dB. This shows that PSD assessment alone is insufficient to determine the fracture type. Therefore, further research should be done, utilizing a more effective method to determine the type of fracture based on the one dimensional ultrasound. In addition to that, one dimensional ultrasound is also beneficial for the determination fracture site by observing the range of attenuation value. Fracture site will have higher attenuation due to the presence of gaps and spaces introduced by the fracture that allows ultrasound to pass through the bone and be further attenuated.

D. Potential of Usage of one dimensional Ultrasound for Bone fracture evaluation in clinical setting

Based on the results presented in this paper, it can be concluded that one dimensional ultrasound imaging has high potential to be used in diagnosing fractures. This is because, the level of ultrasound attenuation in normal and fractured region is different, therefore, the fracture site can be determined precisely. However, the challenge is in making one dimensional ultrasound capable of differentiating many complex fractures, as the current algorithm which is based on power spectral density calculation shows no different value for both type of fractures. It is proposed that this application should be used in diagnosing pregnant women and also

fracture cases in pediatric due to the safe nature of ultrasound wave itself.

ACKNOWLEDGMENT

The authors would like to thank Ministry of Higher Education of Malaysia (MOHE) and Universiti Teknologi Malaysia (UTM) for the financial support under grant 07J20.

REFERENCES

- [1] T. Meling, K. Harboe and K. Soreide, "Incidence of traumatic long bone fractures requiring in hospital management: A prospective age and gender specific analysis of 4890 fractures". *Injury, Int. J. Care Injured* 2009(40): 1212-1219
- [2] C. Mock, M.N. Cherian, "The global burden of musculoskeletal injuries: Challenges and solutions". *Clin Ortop Relat Res.* 2008(16): 2306-2316
- [3] K. Soreide, "Epidemiology of major trauma". *Br. J. Surg.* 2009. 9(7):697-698.
- [4] A. J. Buhr, A.M. Cooke, "Fracture Patterns". *Lancet.* 1959(8):531-536.
- [5] C.M. Court-Brown, B. Ceaser, "Epidemiology of adult fractures: A review." *Injury.* 2006(37): 691-697.
- [6] Copyright image of McGraw-Hill Companies
- [7] M. Doblare, J.M. Garcia, M.J. Gomez, "Modelling bone tissue fracture and healing: A review". *Engineering Fracture Mechanics*, 2004(71): 1809-1840.
- [8] C. Cooper, L.J. Melton, "Hip fractures in the elderly: a world-wide projection". *Osteoporosis Int.* 1992;2:285-9.
- [9] S. Weiner, H.D. Wagner, "The material bone: structure-mechanical function relations". *Ann Rev Mater Sci.* 1998(28):271-298.
- [10] R.A. Robinson, S.R. Elliot, "The water content of bone. The mass of water, inorganic crystals, organic matrix, and "CO₂ space" components in a unit volume of dog bone". *J Bone Joint Surg*, 1957(39A):167-188.
- [11] R. B. Martin, "Porosity and specific surface of bone". *CRC Critical Reviews in Biomedical Engineering*, 1984.
- [12] M. P. Ginebra, J. A. Planell, C. Aparicio, "Structure and mechanical properties of cortical bone". In: *Structural biological materials*. New York: Pergamon Press; 2000. p. 33-71 [chapter 3].
- [13] R.B. Martin, D.B.Burr, N. A. Sharkey. *Skeletal tissue mechanics*. New York: Springer-Verlag; 1998.
- [14] L. White, and G. Duncan, *Medical-Surgical Nursing: An Integrated Approach*, Delmar Thomson Learning, 2002:1000
- [15] W. R. Hendee, R. P. Rossi, *Quality Assurance for Radiographic xray unit and Associated equipments*. US Department of Health, Education and Welfare, FDA Bureau of Radiological Health. 1979.
- [16] P. Hertrich, *Practical Radiography Principles and Application*. Siemens, Germany. 2005. ISBN 3895782106
- [17] A. B. Wolfson, G. W. Hendey, et al, *Harwood-Nuss' Clinical Practice of Emergency Medicine*, Lippincott Williams & Wilkins, 2009 : 254.
- [18] K. K. Shung, (2005). *Fundamentals of Acoustic Propagation. Diagnostic Ultrasound*, CRC Press: 5-37.
- [19] M. Bhandari, R. Mundi, et al, "Low-intensity pulsed ultrasound: Fracture healing." *Indian Journal of Orthopaedics*, 2009. 43(2): 132-140.
- [20] G. Della Rocca, "The science of ultrasound therapy for fracture healing." *Indian Journal of Orthopaedics*, 2009. 43(2): 121-126.
- [21] D. Hans, T. Fuerst, et al. "Bone density and quality measurement using ultrasound." In *Current Opinion in Rheumatology*, 2009. 8(4): 370-375.
- [22] D. P. Hruska, J. Sanchez, et al. "Improved diagnostics through quantitative ultrasound imaging". *Engineering in Medicine and Biology Society*, 2009. EMBC 2009. Annual International Conference of the IEEE.
- [23] B. Madore, P. J. White, et al. "Accelerated focused ultrasound imaging." *IEEE Transactions on Ultrasonics, Ferroelectrics and Frequency Control*, 2009. 56(12): 2612-2623.
- [24] T. L. Tzabo, *Diagnostic Ultrasound Imaging: Inside Out*. Elsevier Academic Press, California, USA. ISBN 0126801452.
- [25] L.C. Gupta, U.C. Sahu, *Diagnostic Ultrasound*, 2nd Edition. Jaypee Brothers Medical Publishers Ltd, 2007. New Delhi India.
- [26] M. I. M. Salim, A. H. Ahmad, et al. "Diagnosis of breast cancer using hybrid magnetoacoustic method and artificial neural network". *Proceedings of the 11th WSEAS international conference on Applied computer science*. Penang, Malaysia, World Scientific and Engineering Academy and Society (WSEAS) 2011: 64-69
- [27] W. R. Hendee, and E. R. Ritenour., *Medical Imaging Physics*, 4th. ed. New York.: Wiley Liss. 2002.
- [28] P. Sprawls, *Physical principles of medical imaging*, 1993. Aspen Publishers.
- [29] P. D. Edmonds and C. L. Mortensen, "Ultrasonic Tissue Characterization for Breast Biopsy Specimen", *Ultrason Imaging*, 1991.13(2):162-185.
- [30] L. Landini and S. Sarnelli, "Evaluation of the Attenuation Coefficient in Normal and Pathological Breast Tissue." *Medical and Biological Engineering and Computing* , 1986. 24:243-247.
- [31] S. G. Ye, K. A. Harasiewicz, C. J. Pavlin, and F. S. Foster, "Ultrasound Characterization of Normal Ocular Tissue in the Frequency Range from 50 MHz to 100MHz". *IEEE Transactions on Ultrasonics, Ferroelectrics, and Frequency Control*, 1995. 42(1):8-14.
- [32] T. Iwamoto, Y. Saijo, N. Hozumi, K. Kobayashi, N. Okada, A. Tanaka, and M. Yoshizawa, "High Frequency Ultrasound Characterization of Artificial Skin". *30th Annual International IEEE EMBS Conference*, August 20-24, 2008. Vancouver, Canada.: IEEE. 2008.
- [33] G. Treece, R. Prager, et al. "Ultrasound attenuation measurement in the presence of scatterer variation for reduction of shadowing and enhancement." *IEEE Transactions on Ultrasonics, Ferroelectrics and Frequency Control*, 2005. 52(12): 2346-2360.
- [34] Kremkau, F. W. *Diagnostic Ultrasound Principles and Instruments*, 6th. ed. Philadelphia.: Saunders. 2002
- [35] Johnson, S. A., Abbott, T., Bell, R., Berggren, M., Borup, D., Robinson, D., Wiskin, J., Olsen, S. and Hanover B. Non-invasive breast tissue characterization using ultrasound speed and attenuation -in vivo validation. *Acoustical Imaging*, 2007. 147-154.
- [36] Berger, G., Laugier, P., Thalabard, J. C. and Perrin, J, Global breast attenuation: control group and benign breast diseases. *Ultrasonic imaging*, 1990. 12: 47-57

Maheza I. Mohamad Salim was born in Selangor, Malaysia, on 26th August 1983. She received an honour degree in Biomedical Engineering (with Distinction) from The University of Malaya, Malaysia in 2006 and her PhD in Biomedical Engineering from Universiti Teknologi Malaysia with specialization in hybrid imaging modality for breast cancer detection in 2012. Currently she is a Senior Lecturer at Faculty of Biosciences and Medical Engineering, Universiti Teknologi Malaysia. Her research interest includes medical physics and instrumentations and cancer research.

Alwin Arul Alexander is currently a Product Development Engineer at Intel Microelectronics Sdn Bhd. This research work was carried out when he was with Faculty of Electrical Engineering, Universiti Teknologi Malaysia, 81310 Johor Bahru, Johor, Malaysia. His research interest including Ultrasound instrumentation and microelectronics.

Sallehuddin Ibrahim is currently an Associate Professor at the Faculty of Electrical Engineering, Universiti Teknologi Malaysia, Johor Bahru, Johor, Malaysia..

Prof. Eko Supriyanto is currently a professor and director of UTM-IJN Cardiovascular Engineering Center, Universiti Teknologi Malaysia. He obtained his PhD in medical electronics from University of Federal Armed Forces, Hamburg, Germany. His research interest is engineering application in medicine. He has more than 150 international publications in the area of medical electronics, medical image processing and medical computing. He has 25 national and international innovation awards and more than 10 patents of biomedical products.